Performance Analysis of UL-DL Decoupled Access in Two-Tier Cellular Heterogeneous Networks

Chuhan Wang

School of Electronic and Information Engineering, Beijing Jiaotong University, Beijing, China.

20211235@bjtu.edu.cn

Abstract. With the advent of the 5th generation mobile communication technology (5G) era, cellular networks are evolving towards highly heterogeneous and ultra-dense network structures, posing challenges for achieving high communication rates. Existing coupled access methods can no longer meet user demands. As a promising solution to this issue, decoupled uplink-downlink access has gained significant attention. This paper investigates the performance of decoupled uplink-downlink access in a two-tier cellular network model. We obtain the analytical expressions of association probabilities, distance distribution, and spectral efficiency of base stations (BSs) when femto-cell BSs are selected for uplink access and macro-cell BSs are selected for downlink access by a user device. Our findings provide insights into the selection of access patterns and decoupled methods for better efficiency and quality of service. Furthermore, our model and approach can guide the design and deployment of next-generation networks to enhance performance.

Keywords: Cellular networks; uplink-downlink decoupled access; association probability; spectral efficiency; stochastic geometry.

1. Introduction

In recent years, cellular networks have grown in importance in wireless communication due to their advantages of heterogeneity, dense deployment, and the ability to handle strong user mobility. However, with the rapid development of technology and information, traditional cellular networks face challenges such as ultra-density limitations and a mismatch between growing user demand for Ultra Reliable Low Latency Communications (uRLLC) and enhanced Mobile Broadband (eMBB), and the network supply capacity. Specifically, in the framework of traditional cellular networks, the received signal power and sources of interference for decoupled uplink (UL) and downlink (DL) access are not the same, leading to significant constraints in coupling efficiency when mobile terminals are limited to being associated with the same BS in the UL and DL directions [1].

To tackle the challenges mentioned above, our research focuses on UL-DL decoupled access in cellular networks. The goal is to separate UL and DL transmissions, allowing each to work independently. This approach enables the use of the strongest signal power for both UL and DL transmissions, as well as improves interference conditions, leading to better transmission signal-to-noise ratio, higher data rates, and lower transmission latency. In simple terms, we propose a two-tier cellular network model that decouples UL and DL transmissions in different BSs, eliminating the interaction between the two. This model can significantly improve the quality of service for users, enable finer management of network resources, support higher resource utilization, and reduce congestion.

Several studies have investigated the feasibility and effectiveness of UL-DL decoupled access. For instance, Smiljkovikj et al. derived the probability of UL/DL association and calculated the throughput of UL and DL BSs [2]. Singh et al. proposed an accurate and tractable model to characterize the UL signal to interference plus noise ratio (SINR) and rate distribution in multi-tier heterogeneous cellular networks for coupled UL-DL offloading [3]. Sattar et al. analyzed the BS distance distribution in a two-tier cellular network using various decoupled methods [4]. Khan et al. explored energy-efficient cell association for traffic offloading in HetNets through the use of UL-DL decoupled access strategy and demonstrated its superiority over the traditional UL-DL coupled access strategy in terms of energy efficiency and interference mitigation [5].

In this paper, we provide a comprehensive analysis of UL-DL decoupled access in cellular networks. We first calculate the probabilities associated with each decoupled case and identify the most widely applicable decoupled methods. Then we analyze the distribution of distances from serving BSs to user devices (UDs) and evaluate the spectral efficiency of the BSs. Our main contributions can be summarized as follows:

1. We propose an analytical framework of a two-tier cellular heterogeneous network based on UL-DL decoupled access.

2. Using the mathematical tools of stochastic geometry, we derive the association probabilities, the distance distribution, and the spectral efficiency of the serving BSs.

3. Through extensive Monte Carlo simulations, we verify the effectiveness of the theoretical analysis results and analyze the performance of UL-DL decoupled access under realistic network conditions.

The remainder of the paper is organized as follows. Section II describes the system model, Section III presents the analysis of the association probabilities, distance distribution, and spectral efficiency, Section IV discusses numerical results and Section V provides a summary of the paper.

2. System Model

In this study, we consider a two-tier cellular heterogeneous network shown in Fig. 1. The network is modeled using a point process denoted Φ_k, which is obtained through a PPP of density λ_k. $k \in \{M, F, U\}$, i.e. the point process includes the sets $\{M, F, U\}$, where M represents the set of macro-cell BSs (MBSs), F represents the set of femto-cell BSs (FBSs), and U represents the set of UDs. The signal transmitting power of the MBS, FBS, and UD are denoted by P_M, P_F, and P_U, respectively.

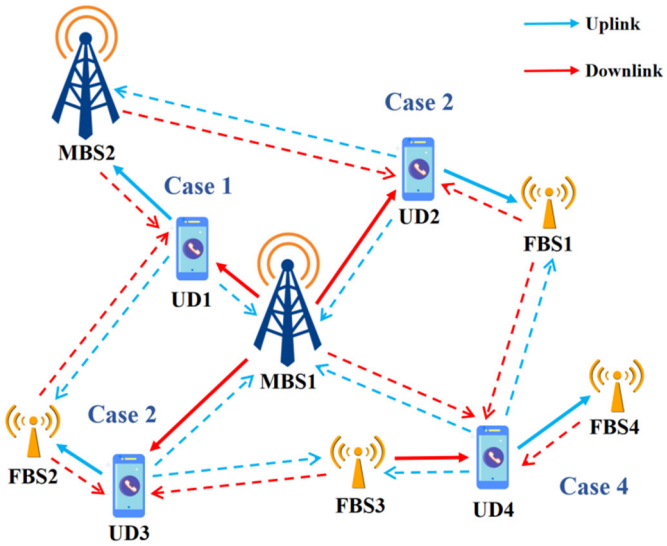


Fig. 1 System Model of UL-DL decoupled access in a two-tier cellular heterogeneous network.

To model the network, we employ a standard path loss model with a path loss exponent of α ($\alpha > 2$). In our analysis, we consider a marked BS and marked UD and assume that they experience only Rayleigh fading with an average of 1 and a transmit power of 1 unless otherwise specified.

In this case, the power received by the typical UD u and emitted by a BS v can be expressed as:

$$S_{v,u,L} = P_v h_{R_{v,u}} R_{v,u}{}^{-\alpha}, \quad (1)$$

where $L \in \{DL, UL\}$, $v \in \{M,F\}$. $R_{v,u}$ represents the distance from a BS v to the typical UD u, and the random variable $h_{R_{v,u}}$ represents the Rayleigh fading at the location of the BS v, which follows an exponential distribution with mean 1, i.e. $h_{R_{v,u}} \sim exp\ (1)$ [6].

For the typical UD u, assume the BS v_1 is the serving BS in decoupled UL access. Then the interference of UL in UL/DL decoupled access is:

$$I_{UL} = \sum_{i \in \Phi_1/u} P_i g_i R_{v_1,i}{}^{-\alpha}. \quad (2)$$

Similarly, assume the BS v_2 is the serving BS of the UD u in decoupled DL access. Then the interference of DL in UL/DL decoupled access is:

$$I_{DL} = \sum_{i \in \Phi_2/v_2} P_i g_i R_{i,u}{}^{-\alpha}, \quad (3)$$

where Φ_1=U, Φ_2={M, F}. We define I_{UL} as the aggregate interference received by all UDs except for the UD u, while I_{DL} is the aggregate interference received from all other BSs (excluding the marked BS for the UD u at node v). The distance between a BS and a UD is subject to a fading effect denoted by g_i, where $g_i \sim exp(1)$. In Fig. 1, the interference of one node to the other is indicated by a dashed arrow.

This paper assumes that the noise power is additive and has value σ^2, but does not generally assume a specific distribution. Thus, the UL SINR is:

$$SINR_{UL} = \frac{P_u h_{R_{v_1,u}} R_{v_1,u}{}^{-\alpha}}{\sigma^2 + I_{UL}}, \quad (4)$$

the DL SINR is:

$$SINR_{DL} = \frac{P_{v_2} h_{R_{v_2,u}} R_{v_2,u}{}^{-\alpha}}{\sigma^2 + I_{DL}}. \quad (5)$$

3. Analysis

The analysis in this paper is organized into three main subsections. Firstly, we derive the association probabilities for decoupled UL and DL access. With these probabilities, we then calculate the distribution of distances between the UD and the serving BSs under the selected scenario (Case 2), and finally evaluate the spectral efficiency of the serving BSs.

3.1 Joint Association Probability

3.1.1 Association Policy

The two-tier heterogeneous model described in Section 2 allows the UD to select at most two different BSs for UL and DL transmission. In this subsection, we investigate how the decision is made to choose between MBS and FBS for UL/DL.

For DL, the UD is associated with the BS that provides the highest average power signal. On the other hand, for UL, the UD is associated with the closest BS. The average received signal power is calculated by averaging the fading of the received signal, as shown in Eq. (1). This method is necessary to avoid ping-pong effects during the association process caused by variations in the signal strength due to fading. The average received signal power for DL and UL are calculated separately as follows:

$$E(S_{v,u,DL}) = P_v R_{v,u}{}^{-\alpha}, \; E(S_{v,u,UL}) = P_u R_{v,u}{}^{-\alpha}, \; v \in \{M, F\}. \quad (6)$$

As shown in the previous equation, the UD always selects the closest BS as the serving BS for UL transmission. For a specific UD, we denote R_v as the shortest distance to the nearest BS v in the set of BSs Φ_v, where $v \in \{M, F\}$. In the decoupled UL access mode, the UD is associated with a MBS if:

$$P_u R_m{}^{-\alpha} > P_u R_f{}^{-\alpha}, \quad (7)$$

the UD is associated with a FBS if:

$$P_u R_m{}^{-\alpha} \leq P_u R_f{}^{-\alpha}. \quad (8)$$

Where R_m represents the shortest distance to the nearest MBS m and R_f represents the shortest distance to the nearest FBS f.

The case in the decoupled DL access is even more complex, as P_v is variable. The UD is associated with a MBS if:

$$P_m R_m{}^{-\alpha} > P_f R_f{}^{-\alpha}, \quad (9)$$

the UD is associated with a FBS if:

$$P_m {R_m}^{-\alpha} \leq P_f {R_f}^{-\alpha}. \quad (10)$$

This description provides a comprehensive understanding of how MBS and FBS are selected in the decoupled UL/DL access.

3.1.2 Derivation of association probabilities

The two-tier heterogeneous model for the association process can result in one of 4 cases. These cases are categorized as follows:

Case 1: UL BS = DL BS = MBS
Case 2: UL BS = FBS, DL BS = MBS
Case 3: UL BS = MBS, DL BS = FBS
Case 4: UL BS = DL BS = FBS

We will discuss each case in detail, but first, we need to derive the probability density function (PDF) and cumulative distribution function (CDF) of r_v using the zero probability of the two-dimensional Poisson point process (PPP) [7]:

$$\mathrm{f}_{R_v}(r) = 2\pi\lambda_v r \cdot exp(-\pi\,\lambda_v r^2)\ (r > 0), \quad (11)$$

$$F_{R_v}(r) = 1 - exp(-\pi\lambda_v r^2)\ (r > 0). \quad (12)$$

In the following analysis, we derive the association probabilities for each of the 4 cases mentioned.

Case 1: UL BS = DL BS = MBS:

Based on the analysis above, the association probability can be expressed as:

$$Pr(Case\ 1) = Pr\left({R_m}^{-\alpha} > {R_f}^{-\alpha}; P_m {R_m}^{-\alpha} > P_f {R_f}^{-\alpha}\right). \quad (13)$$

Considering practical applications, we assume that $P_m > P_f$. The above equation can therefore be rewritten as:

$$Pr(Case1) = Pr\left({R_m}^{-\alpha} > {R_f}^{-\alpha}\right) = \int_0^{\infty} \left(1 - F_{R_f}(r_m)\right) \mathrm{f}_{R_m}(r_m) d\, r_m = \frac{\lambda_M}{\lambda_F + \lambda_M}. \quad (14)$$

(1) Case 2: UL BS = FBS, DL BS = MBS:

Similarly, based on the derivation above, the association probability is:

$$Pr(Case\ 2) = Pr\left({R_m}^{-\alpha} \leq {R_f}^{-\alpha};\ P_m {R_m}^{-\alpha} > P_f {R_f}^{-\alpha}\right). \quad (15)$$

Hence, it is necessary to ensure that the connection between R_m and R_f of the serving MBS and FBS meets the following condition:

$$\frac{P_f}{P_m} {R_f}^{-\alpha} < {R_m}^{-\alpha} \leq {R_f}^{-\alpha}. \quad (16)$$

Thus

$$Pr(Case\ 2) = Pr\left({R_m}^{-\alpha} \leq {R_f}^{-\alpha}\right) - Pr\left(P_m {R_m}^{-\alpha} \leq P_f {R_f}^{-\alpha}\right) = \frac{\lambda_F}{\lambda_F + \lambda_M} - \frac{\lambda_F}{\lambda_F + \varepsilon\lambda_M}, \quad (17)$$

where $\varepsilon = \left(\frac{P_m}{P_f}\right)^{\frac{2}{\alpha}}$.

The derivation for Case 3 and Case 4 is identical to that of Case 1 and Case 2. Due to limitations in space, we will not provide a detailed explanation but will present the results directly below.

(2) Case 3: UL BS = MBS, DL BS = FBS:

$$Pr(Case\ 3) = Pr\left({R_m}^{-\alpha} > {R_f}^{-\alpha}; P_m {R_m}^{-\alpha} \leq P_f {R_f}^{-\alpha}\right) = 0. \quad (18)$$

(3) Case 4: UL BS = DL BS = FBS:

$$Pr(Case\ 4) = Pr\left(P_m {R_m}^{-\alpha} \leq P_f {R_f}^{-\alpha}\right) = \frac{\lambda_F}{\lambda_F + \varepsilon\lambda_M}. \quad (19)$$

3.2 Distance Distributions of the serving BSs

In this subsection, we derive mathematical expressions for the distance distributions of the MBSs and FBSs associated with the typical UD in 4 decoupled methods.

In Case 1, ${R_m}^{-\alpha} > {R_f}^{-\alpha}$. Thus, combining Eq. (11) and Eq. (12), the CCDF of the distance from a UD to its serving MBS can be expressed as:

$$F^{c}_{R_m}\,|_{Case\ 1} = Pr\left(R_m > r | {R_m}^{-\alpha} > {R_f}^{-\alpha}\right) = \frac{Pr\left(R_m > r; {R_m}^{-\alpha} > {R_f}^{-\alpha}\right)}{\mathrm{P}_r(Case\ 1)} = \frac{\int_r^{\infty} exp(-\pi\lambda_F {r_m}^2)\,\mathrm{f}_{R_m}(r_m)dr_m}{\mathrm{P}_r(Case\ 1)}, \quad (20)$$

where $\mathrm{f}_{R_m}(r_m)$ and $\mathrm{P}_r(Case\ 1)$ are given in Eq. (11) and Eq. (13), respectively.The CDF of the distance to the serving BS for Case 1 is:

$$F_{R_m}\,|_{Case\ 1} = 1 - F^{c}_{R_m}\,|_{Case\ 1}, \quad (21)$$

and by simply differentiating this CDF, we derive the PDF of the distance to the serving BS for Case 1:

$$f_{R_m}\,|_{Case\ 1} = \frac{exp(-\pi\lambda_F r^2)\,\mathrm{f}_{R_m}(r)}{\mathrm{P}_r(Case\ 1)}. \quad (22)$$

The derivation of Case 2, Case 3 and Case 4 is analogous to that of Case 1, so the results are given directly below without further elaboration.

In Case 2, the distances between the UD and its serving MBS and FBS satisfy the relation: $\frac{P_f}{P_m} {R_f}^{-\alpha} < {R_m}^{-\alpha} \le {R_f}^{-\alpha}$. Therefore, the CCDF of the distances from the UD to its serving MBS and FBS, respectively, are expressed as:

$$F_{R_m}\,|_{Case\ 2} = \frac{\int_r^{\infty}\left[exp(-\pi\lambda_F {r_m}^2) - exp(-\pi\lambda_F \frac{1}{\varepsilon} {r_m}^2)\right] f_{R_m}(r_m)dr_m}{\mathrm{P}_r(Case\ 2)}, \quad (23)$$

$$F_{R_f}\,|_{Case\ 2} = \frac{\int_r^{\infty}\left[-exp(-\pi\lambda_M \varepsilon {r_f}^2) + exp(-\pi\lambda_M {r_f}^2)\right] f_{R_f}(r_f)dr_f}{\mathrm{P}_r(Case\ 2)}. \quad (24)$$

The PDF of the distances from the typical UD to its serving MBS and FBS, respectively, are denoted as:

$$f_{R_m}\,|_{Case2} = \frac{f_{R_{m1}}(r)}{\mathrm{P}_r(Case2)}, \quad (25)$$

$$f_{R_f}\,|_{Case2} = \frac{f_{R_{f1}}(r)}{\mathrm{P}_r(Case2)}, \quad (26)$$

where

$$f_{R_{m1}}(r) = \left(exp(-\pi\lambda_F \frac{1}{\varepsilon} r^2) - exp(-\pi\lambda_F r^2)\right) f_{R_m}(r)(r > 0), \quad (27)$$

$$f_{R_{f1}}(r) = \left(-exp(-\pi\lambda_M\, \varepsilon r^2) + exp(-\pi\lambda_M r^2)\right) f_{R_f}(r)(r > 0). \quad (28)$$

According to Eq. (18), it is clear that the case of Case 3 does not exist in reality, so

$$f_{R_m}\,|_{Case\ 3} = f_{R_f}\,|_{Case\ 3} = 0. \quad (29)$$

(4) In Case 4, the PDF representation of the distance from the UD to its serving FBS is:

$$f_{R_f}\,|_{Case\ 4} = \frac{exp(-\pi\lambda_M \varepsilon r^2) f_{R_f}(r)}{\mathrm{P}_r(Case\ 4)}. \quad (30)$$

3.3 Spectral Efficiency

Spectral efficiency is the amount of information that can be transmitted per unit of bandwidth [8]. When a wireless communication system is spectral-efficient, it can transmit more data with limited spectrum resources, thus increasing the capacity and efficiency of the network. Therefore, improving spectral efficiency is one of the very important objectives in the design and optimization of wireless communication systems. As Case 2 is the most typical and common decoupled method in practice, the study of BS efficiency in this case is of great practical importance. So in this subsection, we investigate and derive a mathematical expression for the spectral efficiency under Case 2.

According to Shannon's theorem [9], the maximum amount of information that can be transmitted by a wireless channel is denoted as $C = W\,ln(1 + SINR)$, where W is the bandwidth and $SINR$ is the signal-to-noise ratio. Therefore, the spectral efficiency of a serving MBS in the decoupled DL access can be expressed as:

$$\tau(\lambda_M, \alpha) = E[ln(1 + SINR)] = \int_{r>0} E[ln(1 + \frac{P_m h_{r_m} r^{-\alpha}}{\sigma^2 + I_{DL}})] \cdot\ f_{R_m}\,|_{Case\ 2}\ dr. \quad (31)$$

Since for a positive random variable X,

$$E(X) = \int_{t>0} P(X > t)dt, \quad (32)$$

it follows that:

$$\tau(\lambda_M,\alpha)=\int_{r>0}E[ln(1+\frac{P_m h_{R_m} r^{-\alpha}}{\sigma^2+I_{DL}})]\,f_{R_m}\,|_{Case\,2}\,dr$$
$$=\int_{r>0}\int_{t>0}P\left[ln\left(1+\frac{P_m h_{R_m} r^{-\alpha}}{\sigma^2+I_{DL}}\right)>t\right]dt\cdot f_{R_m}\,|_{Case\,2}\,dr$$
$$=\int_{r>0}\int_{t>0}P\left[h_{R_m}>\frac{r^{-\alpha}}{P_m}(\sigma^2+I_{DL})(e^t-1)\right]dt\cdot f_{R_m}\,|_{Case\,2}\,dr. \quad (33)$$

Since the random variable h_{R_m} follows an exponential distribution with mean 1, which we denote as $h_{R_m}\sim$ exp (1), The above equation can be further derived as

$$\int_{r>0}\int_{t>0}E\{exp[-r^{\alpha}{P_m}^{-1}(\sigma^2+I_{DL})(e^t-1)]\}dt\cdot f_{R_m}\,|_{Case\,2}\,dr$$
$$=\int_{r>0}\int_{t>0}exp[-\sigma^2 r^{\alpha}(e^t-1){P_m}^{-1}]E\{exp[-I_{DL}r^{\alpha}(e^t-1){P_m}^{-1}]\}dt\cdot f_{R_m}\,|_{Case\,2}\,dr. \quad (34)$$

Due to the relationship between the Laplace transform and mathematical expectation satisfying

$$L_{I_M}(s)=E_{I_M}[exp(-sI_M)]$$
$$=E_{M,\{g_i\}}\left[exp\left(-s\sum_{i\in M/\{m\}}g_i{R_{i,u}}^{-\alpha}\right)\right]$$
$$=E_{\Phi,\{g_i\}}\left[\prod_{i\in M\setminus\{m\}}E_{g_i}[exp(-sg_i{R_{i,u}}^{-\alpha})]\right]$$
$$=E_{\Phi}\left[\prod_{i\in M\setminus\{m\}}\frac{1}{1+s{R_{i,u}}^{-\alpha}}\right]$$
$$=exp\left(-2\pi\lambda_M\int_r^{\infty}\left(1-\frac{1}{1+sv^{-\alpha}}\right)vdv\right) \quad (35)$$

and

$$L_{I_F}(s)=E_{I_F}[exp(-sI_F)]$$
$$=E_{F,\{g_i\}}\left[exp\left(-s\sum_{i\in F}g_i{R_{i,u}}^{-\alpha}\right)\right]$$
$$=E_{\Phi}\left[\prod_{i\in F}\frac{1}{1+s{R_{i,u}}^{-\alpha}}\right]$$
$$=exp\left(-2\pi\lambda_F\int_0^{\infty}\left(1-\frac{1}{1+sv^{-\alpha}}\right)vdv\right), \quad (36)$$

where I_M and I_F represent for the interference generated by the set of MBSs and the set of FBSs in DL, respectively. $L_{I_M}(s)$ is the Laplace transform of random variable I_M evaluated at s conditioned on the distance to the closest MBS from the origin. $L_{I_F}(s)$ is the Laplace transform of random variable I_F evaluated at s [10]. So the above equation can be converted to:

$$\tau(\lambda_M,\alpha)=\int_{r>0}\int_{t>0}exp(-\sigma^2 r^{\alpha}(e^t-1){P_m}^{-1})\,L_{I_r}(r^{\alpha}(e^t-1){P_m}^{-1})dt\cdot f_{R_m}\,|_{Case\,2}\,dr, \quad (37)$$

where

$$L_{I_r}(r^{\alpha}(e^t-1){P_m}^{-1})=L_{I_M}(r^{\alpha}(e^t-1){P_m}^{-1})\cdot L_{I_F}(r^{\alpha}(e^t-1){P_m}^{-1}), \quad (38)$$

$$L_{I_M}(r^\alpha(e^t-1)P_m{}^{-1}) = exp\left[-2\pi\lambda_M\int_r^\infty\left(1-\frac{v^\alpha}{v^\alpha+r^\alpha(e^t-1)P_m{}^{-1}}\right)vdv\right]$$
$$= exp\left[-2\pi\lambda_M\int_r^\infty\left(1-\frac{v^\alpha}{v^\alpha+r^\alpha(e^t-1)P_m{}^{-1}}\right)vdv\right]$$
$$= exp\left[-\pi\lambda_M r^2 T^{\frac{2}{\alpha}}\int_{T^{-\frac{2}{\alpha}}}^\infty\left(\frac{1}{1+u^{\frac{\alpha}{2}}}\right)du\right], \quad (39)$$

$$L_{I_F}(r^\alpha(e^t-1)P_m{}^{-1}) = exp\left[-\pi\lambda_F r^2 T^{\frac{2}{\alpha}}\int_0^\infty\left(\frac{1}{1+u^{\frac{\alpha}{2}}}\right)du\right], \quad (40)$$

$$T = P_m{}^{-1}(e^t-1). \quad (41)$$

Similarly, the spectral efficiency of a serving FBS in the decoupled UL access can be expressed as:

$$\tau(\lambda_F,\alpha) = \int_{r>0}\int_{t>0} exp(-\sigma^2 r^\alpha(e^t-1)P_f{}^{-1})\, L_{I_U}(r^\alpha(e^t-1)P_f{}^{-1})dt\cdot f_{R_f}\,|_{Case2}\, dr, \quad (42)$$

$$L_{I_U}(r^\alpha(e^t-1)P_f{}^{-1}) = exp\left[-\pi\lambda_U\varepsilon r^2 T^{\frac{2}{\alpha}}\int_{\frac{1}{\varepsilon}T^{-\frac{2}{\alpha}}}^\infty\left(\frac{1}{1+u^{\frac{\alpha}{2}}}\right)du\right]. \quad (43)$$

Where I_U is the interference generated by the set of UDs in UL. $L_{I_U}(s)$ is the Laplace transform of random variable I_U evaluated at s.

4. Numerical Results

4.1 Joint Association Probability

Using the equations for the association probabilities of the 4 decoupled methods discussed in the previous section, we can create a graphical representation of the association probabilities versus λ_F/λ_M. This is depicted in Fig. 2.

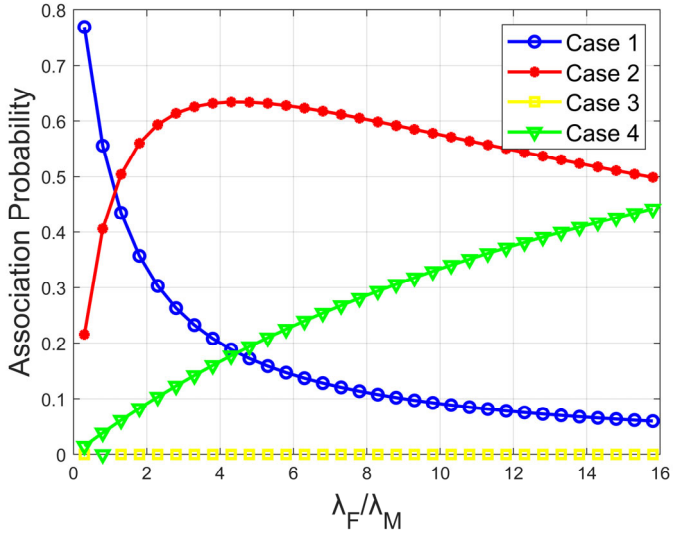


Fig. 2 Graph of the change in association probability for the 4 decoupled methods.

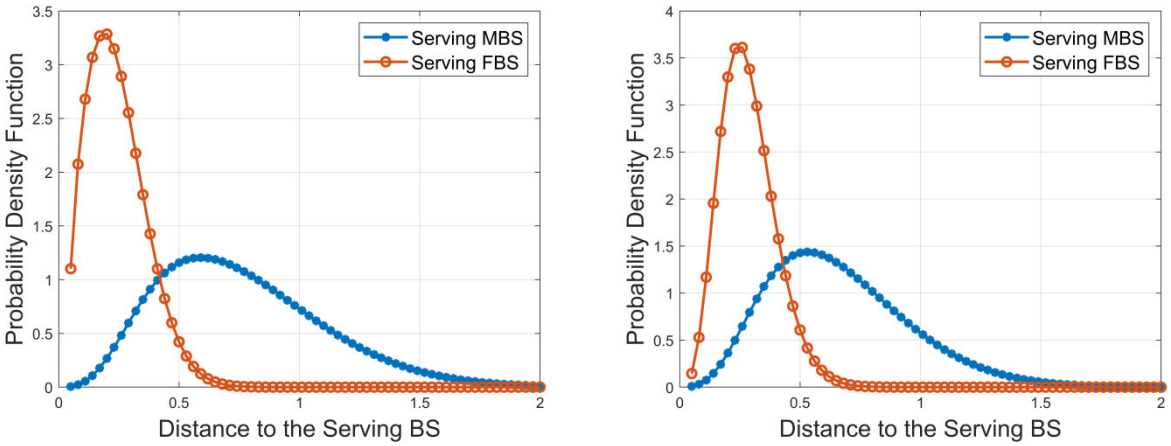
UDs tend to select Case 1 and Case 2 when λ_F/λ_M is less than 1. With an increase in λ_F/λ_M, the probability of selecting Case 1 decreases significantly, while that of Case 2 rises sharply. When λ_F/λ_M exceeds 2, Case 2 becomes the most probable choice for UDs. Furthermore, the probability of selecting Case 4 increases steadily with an increase in λ_F/λ_M but is never higher than that of Case 2 when λ_F/λ_M is below 16.

We examine the association probabilities of UL and DL separately. For UL, the BS selection relies solely on the distance between the BS and the UD, so the closest BS is always chosen. Therefore, when λ_F/λ_M rises, the probability of selecting a FBS as the UL BS increases as the distances from FBSs to the UD decrease. In contrast, DL considers both the distance and transmission power of BSs, where the advantage of distances from the FBSs to the UD becomes more significant as λ_F/λ_M increases. This compensates for the disadvantage of the lower power of FBSs compared to MBSs. Thus, Case 1 exhibits a monotonically decreasing probability curve, while Case 4 shows a monotonically increasing curve. In Case 2, the probability of associating BSs increases continuously with density, whereas the association probability curve shows a declining trend after reaching a peak around 4.

Considering practical circumstances, λ_F/λ_M generally falls within a range that makes Case 2 the most widely used decoupling method. Therefore, it is crucial to investigate the efficiency of BSs under Case 2.

4.2 Distance Distributions of the Serving BSs

Fig. 3 depicts the distance distribution of the UD to its serving BSs under Case 2. The PDF of the distance between the UD and the serving FBS in UL peaks at approximately 0.25 kilometers, ranging from 0 to 0.5 kilometers for both α = 2 and α = 4. In DL, the PDF of the distance between a UD and its serving MBS is spread over a range from 0 to 2 kilometers. As MBSs have an advantage in transmission power, the serving MBS may have a relatively varied distance distribution. Increasing α results in a more concentrated distance distribution of the serving MBS, with a significantly shorter average distance. This is due to the increase in path loss, which requires the UD to be closer to the serving MBS to maintain signal quality, as the MBS transmission power remains constant.



(a) α = 2 (b) α = 4

Fig. 3 Distance distributions of the typical UD to its serving BSs under Case 2.

4.3 Spectral Efficiency

Fig. 4 and Fig. 5 illustrate the correlation between the spectral efficiency of serving BSs and λ_F/λ_M under Case 2. Spectral efficiency is linked to the SINR of the received signal. In UL, as λ_F/λ_M rises, the distance between the UD and the FBS decreases, and signal power increases, resulting in a higher efficiency, but interference from other UDs also grows, causing a rise in UL interference. When λ_F is low, the distance between the serving FBS and the target UD is markedly shortened with an increasing λ_F/λ_M, leading to a rapid increase in spectral efficiency. However, as λ_F increases, the distances between FBS and all UDs become shorter and similar, causing an increase in noise power and a decrease in the rate of efficiency increase.

In DL, the MBS connected to the UD emits the signal, while interference is caused by other MBSs and all FBSs. Increased λ_F/λ_M shortens the distance between FBSs and UDs, leading to higher

interference, but signal power stays the same. Therefore, spectral efficiency decreases continuously as λ_F/λ_M increases.

Increasing the path loss exponent α represents the decrease in received interference and useful signal power, leading to an improved spectral efficiency of the serving FBS and MBS. This is because the attenuation of interference is stronger than that of useful power, resulting in an increase in SINR and spectral efficiency in UL and DL transmissions.

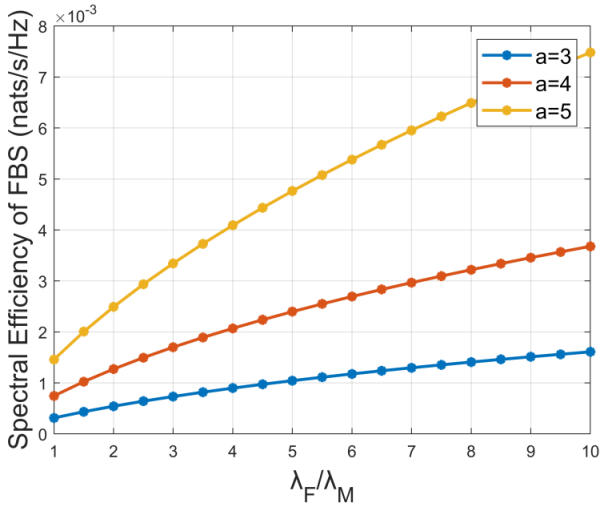


Fig. 4 The correlation between the spectral efficiency of the serving FBS in UL access and the distribution density ratios of FBS and MBS (λ_F/λ_M) under Case 2.

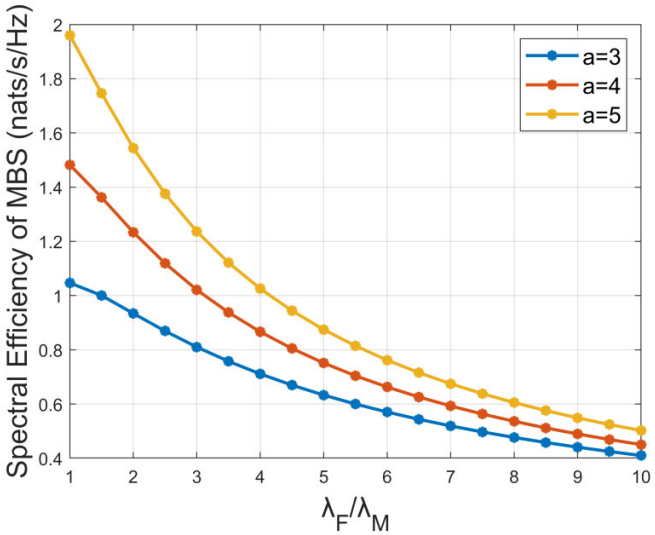


Fig. 5 The correlation between the spectral efficiency of the serving MBS in DL access and the distribution density ratios of FBS and MBS (λ_F/λ_M) under Case 2.

The values of the parameters in the above formulas are listed in Table 1.

Table 1. System Parameters

Parameters	Value
Serving MBS transmit power P_m (dBm)	46
Serving FBS transmit power P_f (dBm)	20
The typical UD transmit power P_u (dBm)	30
MBS distribution density λ_M (nodes/km^2)	0.5
FBS distribution density λ_F (nodes/km^2)	4
UD distribution density λ_U (nodes/km^2)	20
path loss exponent α	4

5. Summary

In this paper, we have done a comprehensive performance analysis for UL-DL decoupled access in a two-tier cellular heterogeneous network. We have derived specific formulas for the distance distribution and the spectral efficiency of the serving BS. The main finding has indicated that the majority of UDs tend to choose the MBS in DL and the FBS in UL. Adjusting λ_F and λ_M can achieve a balance of higher spectral efficiency for both serving FBS and MBS under this decoupled mode, enhancing overall network performance. Moreover, higher α can also boost the spectral efficiency of the serving BS. Our future studies could further improve decoupled UL and DL techniques by exploring other decoupled models, optimal allocation of spectrum resources, and network performance optimization.

References

[1] Boccardi F, Andrews J, Elshaer H, et al. Why to decouple the uplink and downlink in cellular networks and how to do it[J]. IEEE Communications Magazine, 2016, 54(3): 110-117.

[2] Smiljkovikj K, Popovski P, Gavrilovska L. Analysis of the decoupled access for downlink and uplink in wireless heterogeneous networks[J]. IEEE Wireless Communications Letters, 2015, 4(2): 173-176.

[3] Singh S, Zhang X, Andrews J G. Joint rate and SINR coverage analysis for decoupled uplink-downlink biased cell associations in HetNets[J]. IEEE Transactions on Wireless Communications, 2015, 14(10): 5360-5373.

[4] Sattar Z, Evangelista J V C, Kaddoum G, et al. Spectral efficiency analysis of the decoupled access for downlink and uplink in two-tier network[J]. IEEE Transactions on Vehicular Technology, 2019, 68(5): 4871-4883.

[5] Khan H Z, Ali M, Rashid I, et al. Resource allocation for energy efficiency optimization in uplink–downlink decoupled 5G heterogeneous networks[J]. International Journal of Communication Systems, 2021, 34(14): e4925.

[6] F. Baccelli and B. Blaszczyszyn, Stochastic Geometry and Wireless Networks. NOW: Foundations and Trends in Networking, 2010.

[7] Pan S, Han Y, Wei S, et al. A model based on Gauss Distribution for predicting window behavior in building[J]. Building and Environment, 2019, 149: 210-219.

[8] Ngo H Q, Larsson E G, Marzetta T L. Energy and spectral efficiency of very large multiuser MIMO systems[J]. IEEE Transactions on Communications, 2013, 61(4): 1436-1449.

[9] Cabrera J A, Boche H, Deppe C, et al. 6G and the Post-Shannon Theory[J]. Shaping Future 6G Networks: Needs, Impacts, and Technologies, 2021: 271-294.

[10] Andrews J G, Baccelli F, Ganti R K. A tractable approach to coverage and rate in cellular networks[J]. IEEE Transactions on communications, 2011, 59(11): 3122-3134.